

See discussions, stats, and author profiles for this publication at: <https://www.researchgate.net/publication/231370837>

# Color Removal from Wastewater Using Low-Cost Activated Carbon Derived from Agricultural Waste Material

ARTICLE *in* INDUSTRIAL & ENGINEERING CHEMISTRY RESEARCH · MARCH 2003

Impact Factor: 2.59 · DOI: 10.1021/ie020800d

---

CITATIONS

170

---

READS

632

5 AUTHORS, INCLUDING:



**Dinesh Mohan**

Jawaharlal Nehru University

90 PUBLICATIONS **10,443** CITATIONS

SEE PROFILE



**Sarita Sinha**

National Botanical Research Institute - India

109 PUBLICATIONS **4,561** CITATIONS

SEE PROFILE

# Color Removal from Wastewater Using Low-Cost Activated Carbon Derived from Agricultural Waste Material

Kunwar P. Singh,<sup>\*,†</sup> Dinesh Mohan,<sup>†</sup> Sarita Sinha,<sup>‡</sup> G. S. Tondon,<sup>†</sup> and Devlina Gosh<sup>†</sup>

*Environmental Chemistry Division, Industrial Toxicology Research Centre, Post Box No. 80, Mahatma Gandhi Marg, Lucknow 226 001, India, and Environmental Sciences Division, National Botanical Research Institute, Rana Pratap Marg, Lucknow 226 001 (U.P.), India*

An activated carbon was developed from coconut shell fibers, characterized and used for the removal of methylene blue (basic) and methyl orange (acidic) dyes from wastewater successfully. Adsorption studies were carried out at different temperatures, particle size, pH, and adsorbent doses. The adsorption data are correlated with both Langmuir and Freundlich models. The results indicate that the Freundlich model fits the data better as compared to the Langmuir model in terms of regression coefficients. Isotherms have been used to obtain the thermodynamic parameters such as free energy, enthalpy, and entropy of adsorption. The kinetic studies were also conducted, and the adsorption of methylene blue and methyl orange follow the first-order rate equation. Various kinetic parameters such as the mass-transfer coefficient, effective diffusion coefficient, activation energy, and entropy of activation were evaluated to establish the mechanisms. It was concluded that methylene blue adsorption occurs through a film diffusion mechanism at low as well as at higher concentrations, while methyl orange adsorption occurs through film diffusion at low concentration and particle diffusion at high concentrations. The sorption capacity of the developed carbon is comparable to the other available adsorbents, and costwise it is quite cheaper.

## Introduction

Discharge of dye-bearing wastewater into natural streams and rivers from textile, paper, carpet, leather, distillery, and printing industries poses severe problems because dyes impart toxicity to the aquatic life and cause damage to the aesthetic nature of the environment. Considering both volume-discharged and effluent combustion, the wastewater from the textile industry is rated as the most polluting among all industrial sectors.<sup>1</sup> Basic dyes are the brightest class of soluble dyes used by the textile industry.<sup>2</sup> Their tinctorial value is very high; less than 1 ppm of the dye produces an obvious coloration. During the past few years, new and/or stringent regulations coupled with strict enforcement concerning wastewater discharges have been imposed. Therefore, there is a definite need to have a technology, which may work suitably under the above circumstances and should be cost-effective. Various methods of dye/color removal, such as aerobic and anaerobic microbial degradation, coagulation, and chemical oxidation, membrane separation process, electrochemical, dilution, filtration, flotation, softening, and reverse osmosis, have been proposed from time to time.<sup>3–6</sup> However, all of these methods suffered with one or another limitation, and none of these were successful in removing color from the wastewater completely. Although biological treatment processes remove biochemical oxygen demand, chemical oxygen demand, and suspended solids to some extent, they are largely ineffective in removing color from wastewater because most of these are toxic to the organisms used in the process. The coagulation process effectively decolorizes insoluble dyes but fails to work

well with soluble dyes. Photochemical degradation in aqueous solution is likely to progress slowly because synthetic dyes are, in principle, designed to possess a high stability to light. Accordingly, the removal of dyes from effluent in an economic fashion remains a major problem.

Adsorption systems are rapidly gaining prominence as treatment processes that produce good quality effluents that are low in concentration of dissolved organic compounds, such as dyes. Regarding the selection of adsorbents, a literature survey shows that materials such as commercially available activated carbons,<sup>7–10</sup> zeolites,<sup>11,12</sup> etc., have been used in the past for the treatment of textile effluents. Despite the prolific use of activated carbon for the wastewater treatment, carbon adsorption remains an expensive process, and this fact over recent years has prompted a growing research interest into the production of low-cost alternatives to activated carbons. Various low-cost materials have been used for the removal of dyes from time to time. Such materials range from industrial waste to agricultural products. Various workers have exploited substances such as peat,<sup>13,14</sup> bagasse pitch,<sup>15</sup> Fuller's Earth,<sup>16</sup> lignite,<sup>17</sup> coal,<sup>18</sup> activated slag,<sup>19</sup> activated carbon developed from fertilizer waste,<sup>19</sup> bagasse fly ash,<sup>20</sup> activated carbon fibers,<sup>21</sup> wool carbonizing waste,<sup>22</sup> clays,<sup>23</sup> MgCO<sub>3</sub>,<sup>24</sup> perlite,<sup>25</sup> silica,<sup>26</sup> wood meal,<sup>27</sup> activated carbon developed from bamboo,<sup>28</sup> alum sludge,<sup>29</sup> and fly ash<sup>30,31</sup> for this purpose. Other adsorbents and various anaerobic treatment processes are reported in the review articles by Lambert and Graham<sup>32</sup> and Delee et al.<sup>33</sup> However, the problems associated with some of these adsorbents are the regeneration and recovery of the useful materials, which made them unattractive for wider commercial applications. This calls for a research effort to develop some suitable low-cost, efficient indigenous technology capable of removing various dyes/

\* To whom correspondence should be addressed. E-mail: dm\_1967@hotmail.com.

<sup>†</sup> Industrial Toxicology Research Centre.

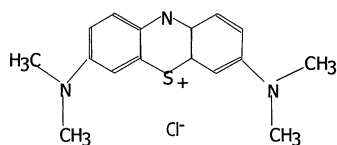
<sup>‡</sup> National Botanical Research Institute.

coloring materials from industrial effluents. This work built upon our earlier publications,<sup>19,20,34–36</sup> in which we have described other novel adsorbents for the removal and recovery of various organic and inorganic pollutants. Continuing our activities in this direction, we have derived a new low-cost activated carbon from coconut shell fibers (a waste material) for the removal of methylene blue (MB) and methyl orange (MO) from wastewater.

## 2. Materials and Methods

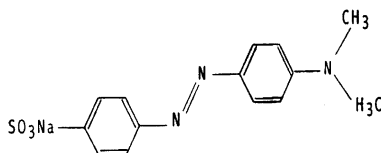
All reagents were of analytical reagent grade chemicals. Stock solutions of the test reagents were made by dissolving MB and MO in doubly distilled water. The pH of the test solutions was adjusted using reagent-grade dilute sulfuric acid (0.1 N) and sodium hydroxide (0.1 N). The chemical formula along with their structures and other properties of the MB and MO dyes are given as follows.

**1.1. MB or Basic Blue 9.** Formula:  $C_{16}H_{18}ClN_3S$ . Molecular weight: 373.90. CI no. 52015.  $\lambda_{\max}$ : 665 nm.



Chemical structure of methylene blue or basic blue 9

**1.2. MO or Acid Orange 52.** Formula weight:  $C_{14}H_{14}N_3NaO_3S$ . Molecular weight: 327.34. C.I. no. 13025.  $\lambda_{\max}$ : 464 nm.



Chemical structure of methyl orange or acid orange 52

**2.1. Equipment.** The pH measurements were made using a pH meter (ELICO model L1-127, India). X-ray measurements were performed using a Philips X-ray diffractometer employing nickel-filtered  $Cu K\alpha$  radiation. The infrared spectrum of the adsorbent was recorded in potassium bromide and Nujol mull in the range of 500–4000  $cm^{-1}$  using a Perkin-Elmer spectrophotometer. The surface area was measured with a Quantasorb model QS-7 surface area analyzer. The porosity and density of the adsorbent were determined using mercury porosimetry and by specific gravity bottles, respectively. The chemical constituents of activated carbon were analyzed following methods of chemical analysis.<sup>37,38</sup> Absorbance measurements were made on a GBC UV–visible spectrophotometer model Cintra 40. The spectrophotometer response time was 0.1 s, and the instrument had a resolution of 0.1 nm. The concentration of both dyes was measured with a 1-cm-light-path cell, with an absorbance accuracy of  $\pm 0.004$  at the maximum wavelength of the dye. The absorbance was found to vary linearly with concentration, and dilutions were made when it exceeds 0.8. Biological degradation of the dyes was also taken into account by running the blank. A Metrohum ion liquid chromatograph (ILC) was used for the estimation of anions.

**2.2. Adsorbent Development.** The raw material, i.e., coconut shell fibers, was collected from Lucknow, India. One part of the coconut fibers was treated with two parts (by weight) of concentrated sulfuric acid, and the same was kept in an oven maintained at 150–165 °C for a period of 24 h. The carbonized material was washed well with double-distilled water to remove the free acid and dried at 105–110 °C for 24 h. The dried material was subjected to thermal activation at different temperatures, viz., 200, 400, 600, and 800 °C for 1 h. The product obtained at a temperature higher or lower than 600 °C exhibited poor adsorption capacity probably (at higher temperature) because of the collapse of surface functional groups. The temperature and time were optimized by observing the surface properties of the activated product obtained by treating the raw material for different intervals of time at the varying temperatures mentioned above. The product so obtained was cooled and sieved to desired particle sizes such as 30–200, 200–250, and 250–300 mesh. Finally, the product was stored in a vacuum desiccator until required.

**2.3. Sorption Procedure.** Sorption studies were performed by the batch technique to obtain rate and equilibrium data. The batch technique was selected because of its simplicity. Batch sorption studies were performed at different temperature, particle size, and adsorbent dose to obtain equilibrium isotherms and data required in the design and operation of column reactors for the treatment of dye-bearing wastewater. For isotherm studies, a series of 100-mL conical flasks were employed. Each conical flask was filled with 50 mL of a dye solution of varying concentrations ( $10^{-5}$ – $10^{-4}$  M) and adjusted to the desired pH and temperature. A known amount of adsorbent was added to each conical flask and agitated intermittently for the desired time periods, up to a maximum of about 48 h. The contact time and other conditions were selected on the basis of preliminary experiments, which demonstrated that the equilibrium was established in 20–24 h. Equilibration for longer times, that is, between 24 and 48 h, gave practically the same uptake. Therefore, a contact period of 24 h was finally selected for all of the equilibrium tests. After this period, the solution was filtered using Whatman No. 42 filter paper and analyzed for the concentration of the dye remaining in the solution by using a spectrophotometer at the corresponding  $\lambda_{\max}$ . The effect of pH was observed by studying the adsorption of dye over a pH range of 2–10. The sorption studies were also carried out at different temperatures, i.e., 30, 40, and 50 °C, to determine the effect of temperature and to evaluate the sorption thermodynamic parameters. Adsorption was also studied at different doses of adsorbent and particle sizes to determine various parameters necessary to design a pilot plant. Exhaustive preliminary investigations reveal that dyes do not interfere in the estimation of each other, and so the adsorbates, i.e., the dyes, were estimated at their adsorption maximum. The dye concentration retained in the adsorbent phase was calculated by using eq 1, where  $C_0$  and  $C_e$  are the initial and equilibrium

$$q_e = (C_0 - C_e)V/W \quad (1)$$

concentrations (M) of dye in solution,  $V$  is the volume (L), and  $W$  is the weight (g) of the adsorbent.

**2.4. Sorption in a Binary System.** Adsorption in multicomponent systems is complicated because of the

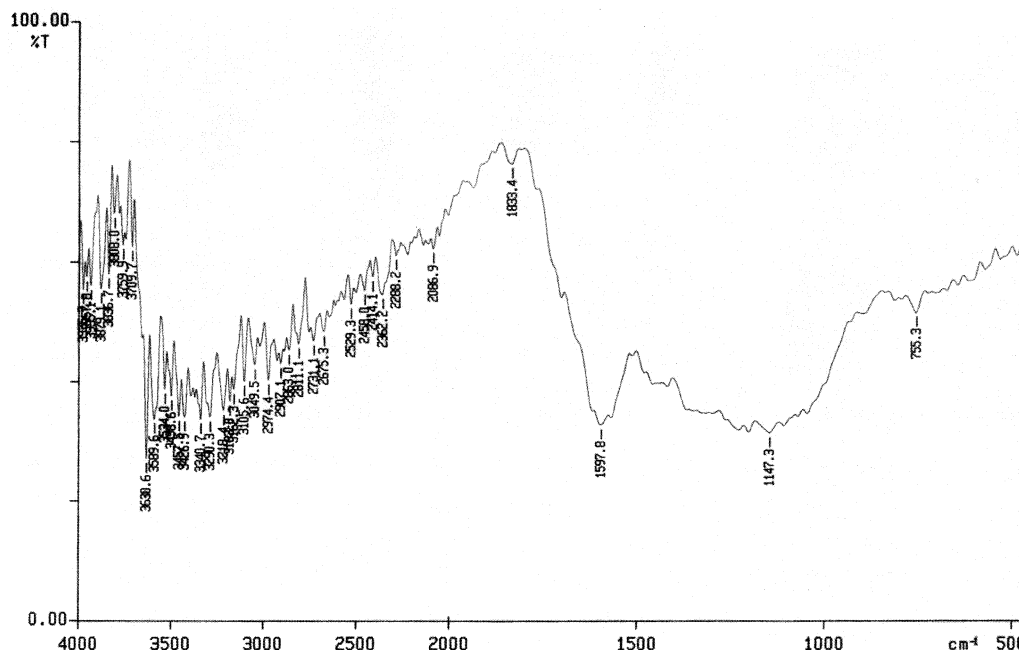


**Figure 1.** IR spectrum of activated carbon derived from coconut shell fibers.

fact that solute–surface interactions are involved. Studies were conducted to delineate the adsorption of MB and MO dyes when present in binary systems. The adsorption studies for MB as well as MO in binary systems were carried out at their optimum pH. A 1:1 ratio was used to determine the effect of interfering dye on the adsorption of MB and MO on the prepared activated carbon. Thus, the interfering effect on dye removal/adsorption was evaluated in terms of the sorption capacity of the prepared carbon. The adsorption data obtained in binary systems were also analyzed for possible agreement with the Langmuir and Freundlich adsorption isotherm models. Further, the adsorption capacities in single and binary systems were compared.

**2.5. Kinetic Studies.** Successful application of the adsorption technique demands innovation of cheap nontoxic, easily available adsorbents of known kinetic parameters and sorption characteristics. Foreknowledge of optimal conditions would herald a better design and modeling of the process. Thus, the effects of some major parameters, viz., contact time, amount, and particle size of the adsorbent, on the adsorption of dyes were studied. For kinetic study investigations, the bath technique was selected because of its simplicity. A number of stoppered flasks (100-mL capacity) containing a 50-mL solution of each dye were placed in a thermostat shaking assembly. When the desired temperature was reached, a known amount of activated carbon was added into each flask and the solutions were agitated by mechanical shaking. At predecided intervals of time, the solutions of the specified flask were separated from the activated carbon and analyzed for the uptake of dye at their respective  $\lambda_{\max}$ .

### 3. Results and Discussion

**3.1. Characterization.** For characterization of the prepared activated carbon, samples (1.0 g) were stirred with deionized water (100 mL, pH 6.8) for 2 h and left for 24 h in an airtight stoppered conical flask. A lowering of the pH was observed. The carbon is quite stable in water, salt solutions, acids, bases, and organic

solvents. The different chemical constituents of activated carbon prepared from coconut shell fibers are as follows: surface area, 978 m<sup>2</sup>/g; pH 5.4; bulk density, 0.356 g/cm<sup>3</sup>; ash, 62%; C, 76.38%; H, 1.95%; N, 0.38%; LOI, 24%.

The IR spectrum of activated carbon (Figure 1) indicated weak and broad peaks in the region 3853–453 cm<sup>-1</sup>. Approximate FTIR band assignments indicated the presence of carbonyls, carboxyls, lactones, and phenols. The 188–1540-cm<sup>-1</sup> band was associated with the C=O stretching mode in carbonyls, carboxylic acids, and lactones, while the 1440–1000-cm<sup>-1</sup> band was assigned to the C=O stretching and O–H bending modes such as phenols and carboxylic acids. Although some inference can be made about the surface functional groups from IR spectra, the weak and broad bands do not provide any authentic information about the nature of surface oxides. The data, however, indicate the presence of some surface groups on the adsorbent material.

The X-ray diffraction analysis of activated carbon does not show any peak (figure not given in the manuscript), thereby indicating the amorphous nature of the carbon prepared from coconut shell fibers. Scanning electron microscopy (SEM) photographs (Figure 2) at 4000× magnification clearly revealed the surface texture and different levels of porosity in the prepared activated carbon under study. It is evident that the carbon particles are in the form of spherical particles of a wide range of sizes. The larger particles seem to be made up of aggregates of the smaller ones.

**3.2. Sorption Studies. 3.2.1. Determination of the Equilibrium Time.** The contact time and other conditions were selected on the basis of preliminary experiments that demonstrated that the equilibrium was established in 20–24 h, as can be seen from the results in Figure 3a,b. Equilibration for longer times, that is, between 24 and 48 h, gave practically the same uptake. Therefore, the contact period was 24 h in all equilibrium tests. After this period, the solution was filtered using Whatman No. 42 filter paper and analyzed for the concentration of the dye remaining in the solution by



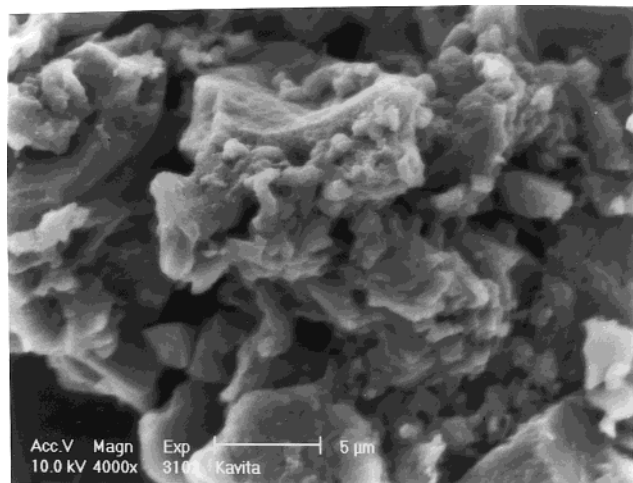


**Figure 2.** SEM photographs of activated carbon at 4000 $\times$  magnification.

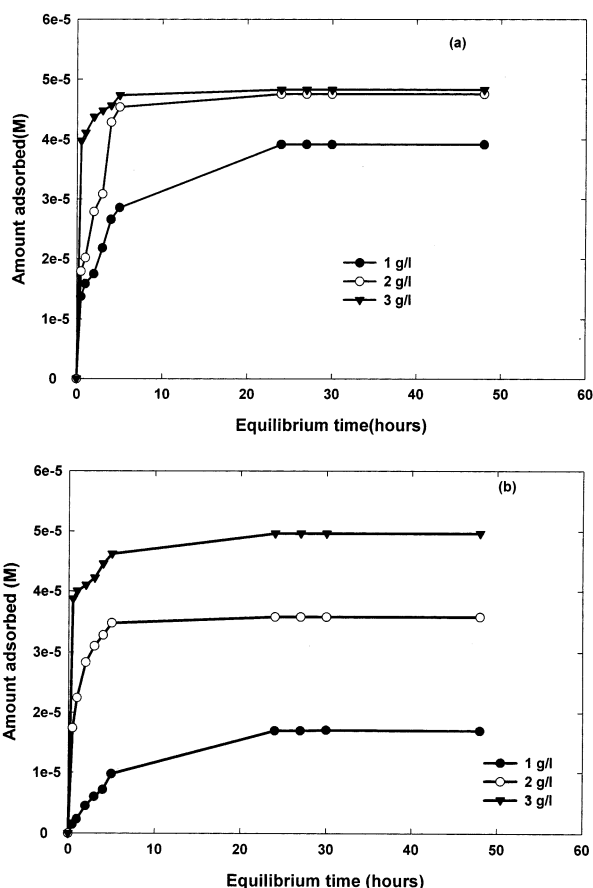


**Figure 3.** Effect of the contact time on the rate of adsorption of (a) MB and (b) MO by activated carbon at different adsorbent concentrations at 30 °C and an adsorbate concentration of  $5 \times 10^{-5}$  M.

using a spectrophotometer. The distribution of dyes between the adsorbent and the dye solution, when the system is in a state of equilibrium, is important to establish the capacity of the adsorbent for the dyes. The effect of the amount of adsorbents on the removal of dyes is given in Table 1. The uptake increases with an increase in the amount of the adsorbent material (Table 1). There is a substantial increase in the adsorption when the carbon dosage increases from 1 to 2 g/L, while the increase on introduction of an additional 1 g/L of carbon is not significant. From this point of view, the

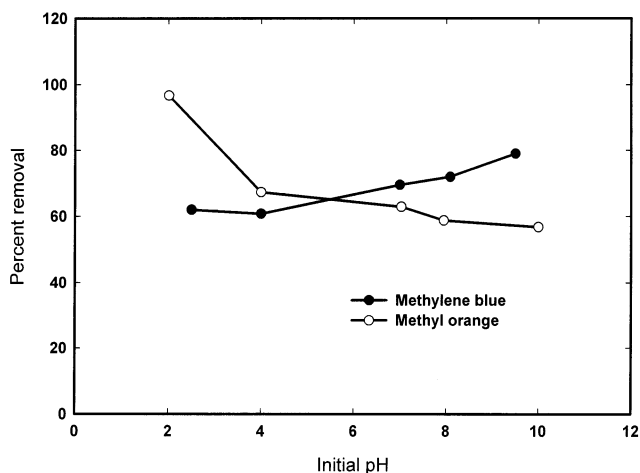


**Figure 4.** Effect of the pH on the adsorption of MB and MO by activated carbon at 30 °C and an adsorbate concentration of  $5 \times 10^{-5}$  M.

**Table 1.** Effect of the Amount of Activated Carbon on the Rate of Uptake of MB and MO (Initial Concentration of Dye,  $5 \times 10^{-5}$  M; Particle Size = 30–200 mesh; Temperature =  $30 \pm 1$  °C) on Prepared Carbon

dye	amount of adsorbent (g/L)	amount adsorbed in the first hour (mol)	$t_{50}$ (h)
MB	1.0	$1.58 \times 10^{-5}$	2.8
	2.0	$2.01 \times 10^{-5}$	1.8
	3.0	$4.11 \times 10^{-5}$	0.4
MO	1.0	$0.23 \times 10^{-5}$	4.8
	2.0	$2.24 \times 10^{-5}$	0.6
	3.0	$4.00 \times 10^{-5}$	0.4

amount of carbon has been kept at 2 g/L of carbon in all of the subsequent studies. The adsorption studies were carried out at different temperatures, adsorbent doses, and particle sizes to determine the adsorption isotherms and the necessary parameters to set up pilot plants on a large scale and are discussed below.

**3.2.2. Effect of pH.** The pH is the most important factor affecting the adsorption process. To study the influence of pH on the adsorption capacity of prepared activated carbon, experiments were performed using various initial pH's varying from 2 to 10. The variation in the adsorption of MB and MO over a broad pH range of 2–10 is depicted in Figure 4. It is seen that the higher the pH, the higher the amount of MB adsorbed on activated carbon. The percent removal of MB is constant in the pH range of 2–4. Upon a further increase in the pH, the adsorption increases and was found to be a maximum at pH 10.0. Keeping in mind the effluent pH from textile and other industries and to correlate the removal process with adsorption, the optimum pH is chosen as 6.0 for further adsorption studies. Basically, MB and other cationic dyes produce an intense molecular cation ( $C^+$ ) and reduced ions ( $CH^+$ ). The base peak in MB was due to  $C^+-CH_3$ .

On the other hand, the percent adsorption of MO (Figure 4) is more at pH 2 and a sharp decrease is observed as the pH increases from 2 to 4. Upon a further increase in pH ( $>4$ ), the adsorption decreases but the decrease is not very sharp, and at pH 10 the adsorption is found to be a minimum. As such, all of the subsequent adsorption studies on MO were carried out in an acidic range and pH 4 was selected as the optimum. The adsorption of MO at different pH's with the variation of the adsorbent dose was also carried out. The removal efficiency of the activated carbon increases with an

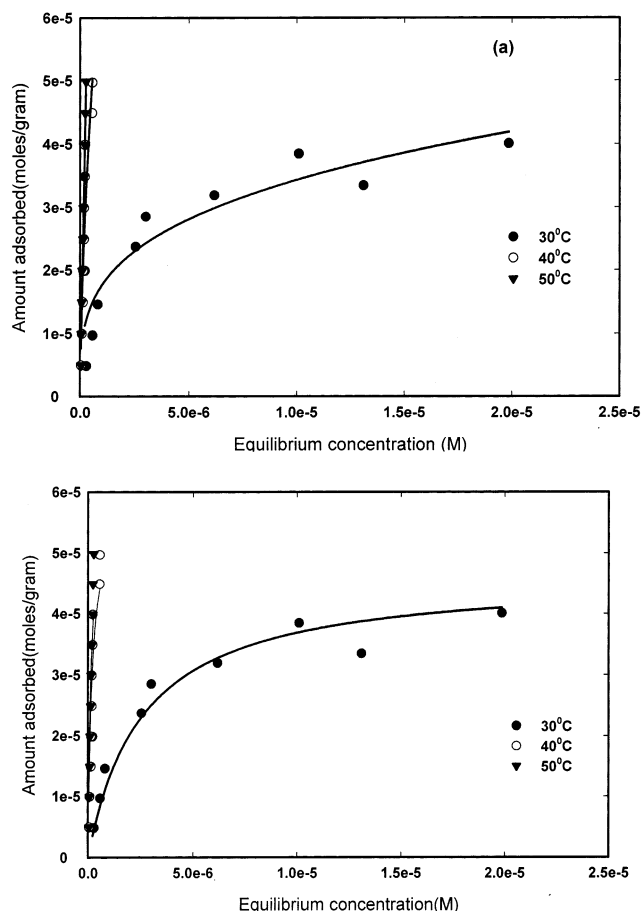


**Figure 5.** Adsorption of MB on activated carbon derived from coconut shell fibers at different temperatures and pH 6.0. Solid lines represent the fitting of data by (a) Freundlich and (b) Langmuir isotherms.

increase in the adsorbent dose, while the removal pattern at different pH's remains the same.

**3.2.3. Effect of the Temperature.** The adsorption isotherms were determined for various dye-adsorbent systems. The removal of MB and MO has been studied at 30, 40, and 50 °C to determine the adsorption isotherms and thermodynamic parameters, which are presented in Figures 5 and 6, respectively. The extent of adsorption of dyes is found to increase with temperature (Tables 2 and 3), indicating the process to be endothermic in nature. All of the isotherms are positive, regular, and concave to the concentration axis. The uptake of both of the selected dyes on prepared low-cost activated carbon is almost 100% at low concentration of the adsorbates while the same decreases when the adsorbate concentrations are higher. The increase in the uptake of dyes with temperature may be due to the enhanced rate of intraparticle diffusion of the adsorbate because the diffusion is an endothermic process. The increase in the adsorption behavior suggests that active surface centers available for adsorption have increased with temperature. This may also be a result of an increase in the mobility of the large dye ion with temperature. An increasing number of molecules may also acquire sufficient energy to undergo an interaction with active sites at the surface. Furthermore, increasing the temperature may produce a swelling effect within the internal structure of the carbon, enabling large dyes to penetrate further, as found by Gupta et al.<sup>19</sup> for the adsorption of basic dye on activated carbon and activated slag.

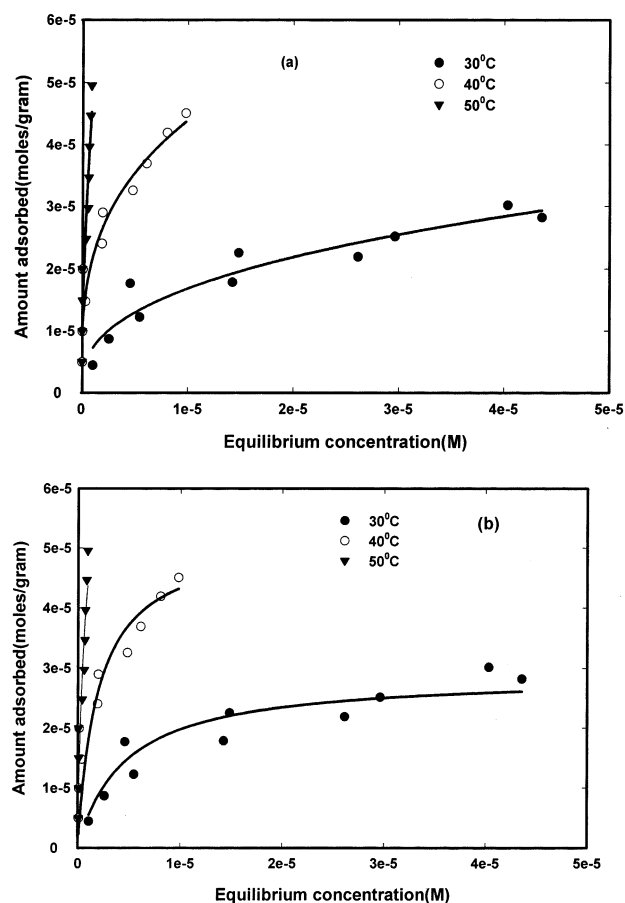


**Figure 6.** Adsorption of MO on activated carbon derived from coconut shell fibers at different temperatures and pH 4.0. Solid lines represent the fitting of data by (a) Freundlich and (b) Langmuir isotherms.

**Table 2. Nonlinear Freundlich Isotherm Constants for MB and MO Adsorption on Activated Carbon Derived from Coconut Shell Fibers at Different Temperatures**

temp (°C)	MB			MO		
	$K_F$ (mol/g)	$1/n$	$R^2$	$K_F$ (mol/g)	$1/n$	$R^2$
30	0.009	0.2883	0.8359	0.0013	0.3761	0.9083
40	0.2036	0.5764	0.8525	0.0016	0.3114	0.9262
50	75.58	0.9380	0.9860	0.2073	0.6068	0.9020

In the surface adsorption studies, the relationship between the solution concentration and the species uptake can be described in terms of either a Freundlich- or Langmuir-type isotherm; therefore, the data were evaluated using linear and nonlinear Langmuir and Freundlich isotherms<sup>34,39</sup> (eqs 2–5).

**Langmuir Isotherm.** The Langmuir equation may be written as

$$q_e = \frac{Q^0 b C_e}{1 + b C_e} \quad (\text{nonlinear form}) \quad (2)$$

$$\frac{C_e}{q_e} = \left( \frac{1}{Q^0 b} \right) + \left( \frac{1}{Q^0} \right) C_e \quad (\text{linear form}) \quad (3)$$

where  $q_e$  is the amount of solute adsorbed per unit weight of adsorbent (mol/g),  $C_e$  is the equilibrium concentration of the solute in the bulk solution (mol/L),  $Q^0$  is the monolayer adsorption capacity (mol/g), and  $b$  is the constant related to the free energy of adsorption

**Table 3. Nonlinear Langmuir Isotherm Constants for MB and MO Adsorption on Activated Carbon Derived from Coconut Shell Fibers at Different Temperatures**

temp (°C)	MB			MO		
	$Q^0 \times 10^5$ (mol/g)	$b \times 10^{-5}$ (L/mol)	$R^2$	$Q^0 \times 10^5$ (mol/g)	$b \times 10^{-5}$ (L/mol)	$R^2$
30	4.60	3.9	0.7515	2.88	2.17	0.8865
40	5.74	60.02	0.8471	5.16	5.19	0.7534
50	8.94	81.16	0.8210	7.17	16.23	0.8621

**Table 4. Nonlinear Freundlich Parameters for MB and MO Adsorption on Activated Carbon Derived from Coconut Shell Fibers at Different Particle Sizes**

particle size (mesh)	MB			MO		
	$K_F$ (mol/g)	$1/n$	$R^2$	$K_F$ (mol/g)	$1/n$	$R^2$
30–200	0.009	0.2833	0.9031	0.0013	0.3761	0.9083
200–250	0.0468	0.5260	0.7571	0.0129	0.5357	0.8231
250–300	5.3558	0.8447	0.8605	0.2040	0.5549	0.9168

**Table 5. Nonlinear Langmuir Isotherm Constants for MB and MO Adsorption on Activated Carbon Derived from Coconut Shell Fibers at Different Particle Sizes**

particle size (mesh)	MB			MO		
	$Q^0 \times 10^5$ (mol/g)	$b \times 10^{-5}$ (L/mol)	$R^2$	$Q^0 \times 10^5$ (mol/g)	$b \times 10^{-5}$ (L/mol)	$R^2$
30–200	4.60	3.90	0.9545	2.88	2.17	0.8865
200–250	4.90	23.06	0.7081	4.72	1.60	0.8619
250–300	5.24	25.71	0.6597	4.98	3.17	0.9076

( $b \propto e^{-\Delta G/RT}$ ). It is the reciprocal value of the concentration at which half the saturation of the adsorbent is attained.

**Freundlich Isotherm.** The Freundlich equation may be written as

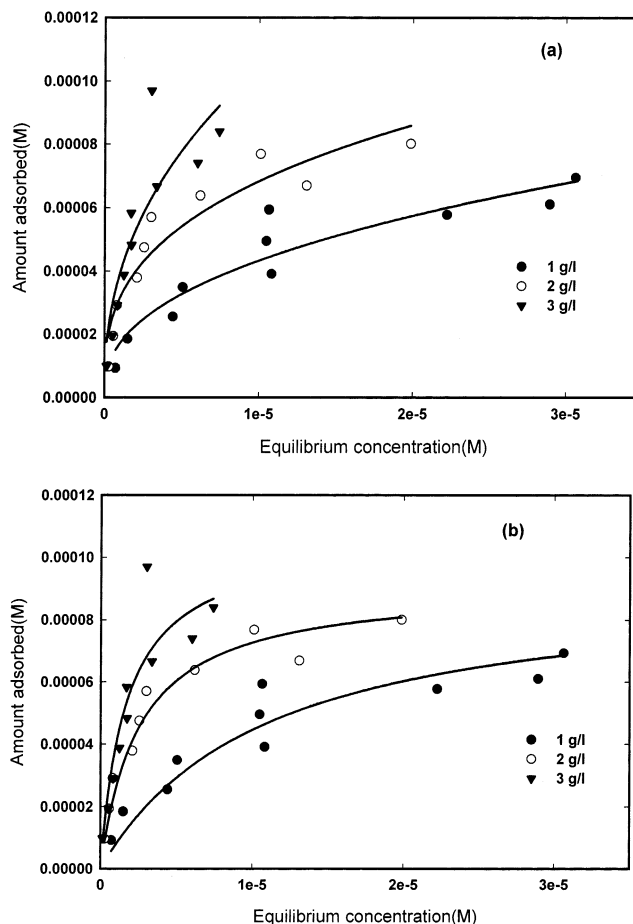
$$q_e = K_F C_e^{1/n} \quad (\text{nonlinear form}) \quad (4)$$

$$\log q_e = \log K_F + \frac{1}{n} \log C_e \quad (\text{linear form}) \quad (5)$$

where  $q_e$  is the amount of solute adsorbed per unit weight of adsorbent (mol/g),  $C_e$  is the equilibrium concentration of the solute in the bulk solution (mol/L),  $K_F$  is the constant indicative of the relative adsorption capacity of the adsorbent (mol/g), and  $1/n$  is the constant indicative of the intensity of the adsorption.

Figures 5 and 6 show the applicability of both models over a wide range of concentrations. A detailed analysis of the regression coefficients showed that Langmuir and Freundlich models adequately described the adsorption data at different temperatures, but the data are slightly better fitted by the Freundlich adsorption isotherms (Figure 9). The Langmuir and Freundlich parameters as calculated from the nonlinear form at different temperatures are given in Tables 2 and 3, respectively. It can be seen from Table 3 that the values of  $Q^0$  are found to be higher in the case of the carbon–MB system. The values of the Freundlich constant,  $K_F$ , follow the same pattern as  $Q^0$  because  $K_F$  also indicates the relative adsorption capacity.

**3.2.4. Effect of the Particle Size.** The effects of the particle sizes (30–200, 200–250, and 250–300 mesh) on the rate of uptake of MB and MO are presented in Tables 4 and 5, respectively. The uptake of dyes on the prepared activated carbon increases with decreasing particle size of the adsorbent. A detailed analysis of the regression coefficients showed that both the Langmuir

**Figure 7.** Adsorption of MB on activated carbon derived from coconut shell fibers at different carbon doses and pH 6.0. Solid lines represent the fitting of data by (a) Freundlich and (b) Langmuir isotherms.

and the Freundlich models adequately described the adsorption data, but the data are better modeled by the Freundlich isotherm (figures omitted for brevity). This relationship clearly demonstrates the advantage of powdered adsorbent over granular form from a kinetic viewpoint, indicating that the external transport limits the rate of adsorption in these cases. No trend was found for  $K_F$  for the uptake of both of the dyes on activated carbon.

### 3.2.5. Effect of the Adsorbent Concentrations.

The effect of the amount of adsorbent on the rate of uptake of MB and MO is shown in Figures 7 and 8. The uptake of the dyes increases with an increase in the amount of the adsorbent material (table omitted for brevity). The adsorption of both of the dyes increases significantly (from 69 to 80% and from 26 to 56%) when the adsorbent dose increases from 5 to 10 g/L, but upon a further increase in the adsorbent dose, the removal efficiency does not change in that significant ratio. In the case of MO, the adsorption increases by twofold when the adsorbent dose increases twofold. Keeping this in mind, the amount of activated carbon has been kept at 2.0 g/L in all of the adsorption studies. Nonlinear and linear forms of both of the isotherms also fit the adsorption data quite well in the broad range of concentrations. Similarly to the effect of the temperature as well as the particle size, the nonlinear Freundlich adsorption isotherm modeled the data better as compared to the Langmuir adsorption isotherm (Figure 9).

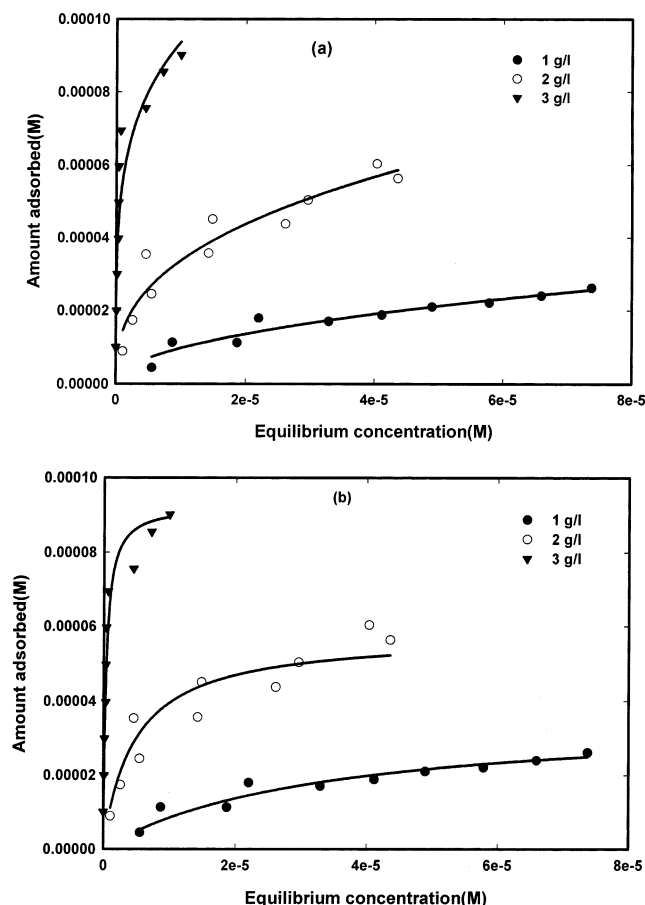


**Figure 8.** Adsorption of MO on activated carbon derived from coconut shell fibers at different carbon doses and pH 4.0. Solid lines represent the fitting of data by (a) Freundlich and (b) Langmuir isotherms.

The essential characteristic of a Langmuir isotherm can be expressed in terms of a dimensionless constant separation factor,  $R_L$ , which is defined by Weber and Chakravorti<sup>40</sup> and was applied earlier by us<sup>19,20,34–36</sup> on different systems. The dimensionless separation factor  $R_L$  was determined at different temperatures, particle sizes, and adsorbent doses in the broad concentration range. In all of the cases, the values of  $R_L$  were found to be less than 1 and greater than 0, indicating the favorable adsorption of both the MB and MO on activated carbon derived from coconut shell fibers.

**3.2.6. Thermodynamic Parameters.** Thermodynamic parameter, i.e., free energy ( $\Delta G^\circ$ ), enthalpy ( $\Delta H^\circ$ ), and entropy ( $\Delta S^\circ$ ), changes were also calculated using eqs 6–8 and are given in Table 6, where  $K_1$  and

$$\Delta G^\circ = -RT \ln K_1 \quad (6)$$

$$\Delta H^\circ = -R \left( \frac{T_2 T_1}{T_2 - T_1} \right) \ln \frac{K_2}{K_1} \quad (7)$$

$$\Delta S^\circ = \frac{\Delta H^\circ - \Delta G^\circ}{T} \quad (8)$$

$K_2$  are the Langmuir constants which are the same as  $b_1$  and  $b_2$  corresponding to temperatures at 30 and 40 °C. The negative values of  $\Delta G^\circ$  indicate the feasibility and spontaneous nature of MB and MO adsorption on activated carbon derived from coconut shell fibers. The change in enthalpy  $\Delta H^\circ$  for both of the dyes on prepared

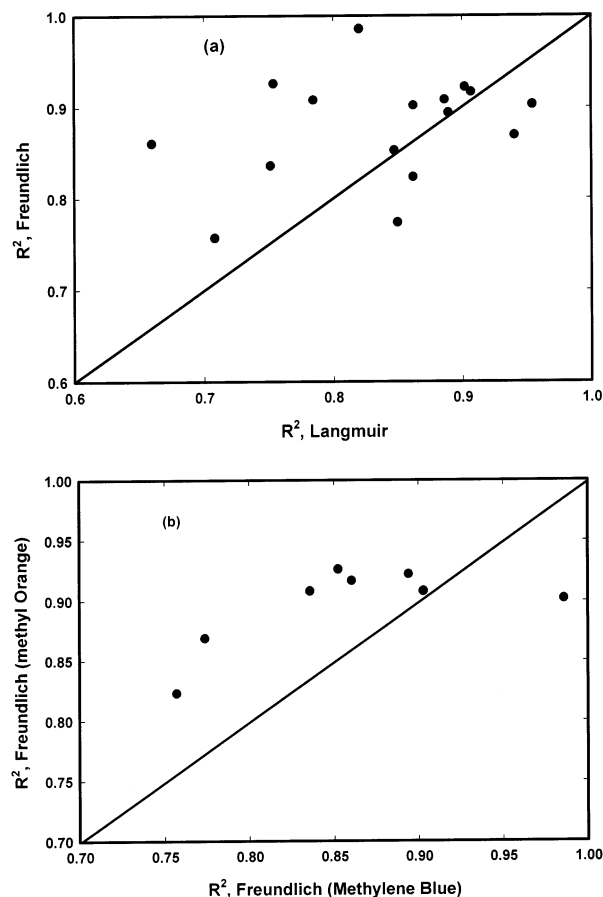


**Figure 9.** Comparative evaluation of (a) Langmuir and Freundlich regression coefficients for MB and MO and (b) Freundlich regression coefficients for MB and MO dyes.

**Table 6. Thermodynamic Parameters for the Adsorption of MB and MO on Activated Carbon Derived from Coconut Shell Fibers**

dye	$-\Delta G$ (kJ/mol)			$\Delta H$ (kJ/mol)	$\Delta S$ [kJ/(mol K)]
	10 °C	25 °C	40 °C		
MB	32.43	40.61	42.72	120.95	0.2921
MO	30.95	34.24	38.40	82.15	0.1689

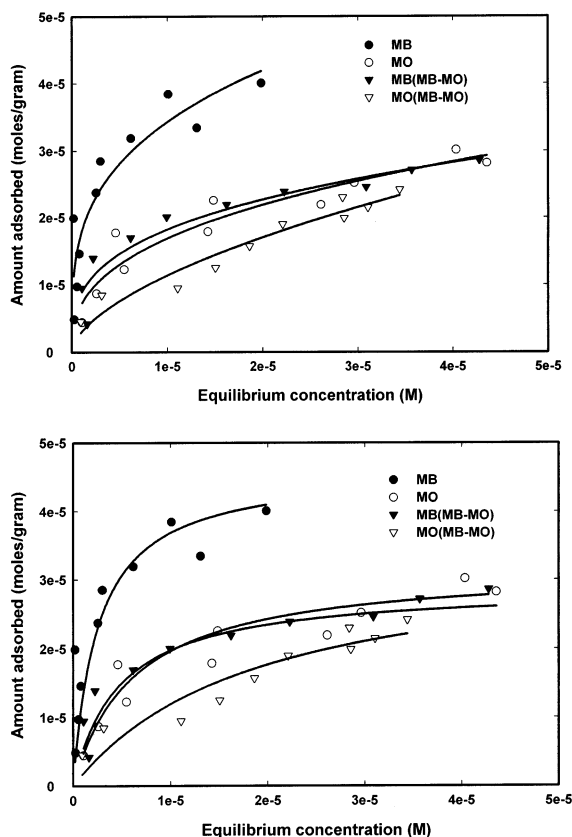
carbon was found to be positive (Table 6). The positive values confirm the endothermic nature of adsorption. These values are consistent with the results presented in Tables 2 and 3. The positive values of the entropy change show the increased randomness at the solid/solution interface with some structural changes in the adsorbate and adsorbent and an affinity of the adsorbent toward MB and MO.

**3.2.7. Bisolute Adsorption Studies.** The adsorption of dyes in a binary system was carried out at pH 6.0 and 30 °C. The concentration range of  $1.0 \times 10^{-5}$ – $1.0 \times 10^{-4}$  M was investigated, and a ratio of 1:1 was used to determine the effect on the adsorption of MB and MO in the presence of each other. The Freundlich and Langmuir adsorption isotherms for MB and MO in a binary system are presented in Figure 10a,b. Both Langmuir and Freundlich isotherms could adequately describe the data over the entire range of concentration, and corresponding parameters are presented in Table 7. A detailed analysis of the regression coefficients showed that Langmuir and Freundlich models adequately described the adsorption data, but the data are better fitted by the Freundlich isotherm for both of the dyes in single as well as binary systems, as can be seen



**Table 7. Freundlich and Langmuir Isotherm Constants for Single and Binary Adsorption of MB and MO on Activated Carbon Developed from Coconut Shell Fibers**

system	Freundlich constant			$K_F^{\text{mix}}/K_F$	Langmuir constant			
	$K_F$ (mol/g)	$1/n$	$R^2$		$Q^0 \times 10^5$ (mol/g)	$b \times 10^{-5}$ (L/mol)	$R^2$	$Q^{\text{mix}}/Q^0$
MB alone	0.009	0.28	0.8359	0.77	4.60	3.90	0.7515	0.68
MB(MB–MO)	0.007	0.32	0.9706		3.17	1.62	0.8837	
MO alone	0.0013	0.38	0.9083	0.71	2.88	2.17	0.8865	0.96
MO(MB–MO)	0.0093	0.58	0.9864		2.78	0.06	0.8748	

**Figure 10.** Single and binary adsorption of MB and MO on activated carbon derived from coconut shell fibers at 30 °C and pH 6.0. Solid lines represent the fitting of data by (a) Freundlich and (b) Langmuir isotherms.

from Figure 9. Although the Freundlich and Langmuir constants  $K_F$  and  $Q^0$  have different meanings, this led to the same conclusion about the correlation of the experimental data with the sorption model. The basic difference between  $K_F$  and  $Q^0$  is that the Langmuir isotherm assumes free-energy adsorption to be independent of both the surface coverage and the formation of a monolayer whereas the solid surface reaches saturation while the Freundlich isotherm does not predict saturation of the solid surface by the adsorbate; therefore, the surface coverage is mathematically unlimited. In conclusion,  $Q^0$  is the monolayer adsorption capacity, while  $K_F$  is the relative adsorption capacity or adsorption power.

The effect of the ionic interaction<sup>34,36</sup> on the sorption process may also be represented by the ratio of the sorption capacity for one dye in the presence of another,  $Q^{\text{mix}}$ , to the sorption capacity for the same dye when it is present alone in the solution,  $Q^0$ , such that, for  $Q^{\text{mix}}/Q^0 > 1$ , the sorption is promoted by the presence of another dye, for  $Q^{\text{mix}}/Q^0 = 1$ , there is no observable net interaction, and for  $Q^{\text{mix}}/Q^0 < 1$ , sorption is suppressed by the presence of another dye.

The values of  $Q^{\text{mix}}/Q^0$  are found to be less than 1, as presented in Table 7. These results are consistent with the sorption isotherms obtained for MB and MO in the absence and presence of each other. The prepared activated carbon followed the same trend; that is,  $Q^{\text{mix}}$  decreased in the following order for the adsorption of MB(II) < MB(MB–MO) < MO < MO(MB–MO) in a binary system. Overall, it may be concluded that the adsorption capacity of activated carbon for MB and MO decreases in binary systems.

**3.3. Kinetic Studies.** The effect of the amount of adsorbent on the rate of uptake of MB and MO is shown in Figure 3. The uptake increases with an increase in the amount of the adsorbent material (Table 1). There is a substantial increase in the adsorption when the carbon dosage increases from 1 to 2 g/L, while the increase upon introduction of an additional 1 g/L of carbon is not significant. Keeping this in mind, the amount of carbon has been kept at 2 g/L in all of the subsequent kinetic studies. Further, the half-life of the process ( $t_{50}$ ) decreases with an increase in the amount of adsorbent, confirming that the rate of adsorption is dependent on the amount of carbon. Preliminary investigations on the rate of uptake of MB and MO on activated carbon indicated that the processes are quite rapid and typically 40–50% of the ultimate adsorption occurs within the first hour of contact (Figure 3 and Table 1). This adsorption subsequently gives way to a very slow approach to equilibrium, and in 20–24 h, saturation is reached. The kinetics of the removal of MB and MO has also been studied at 30, 40, and 50 °C and is presented in Figure 11. The extent of adsorption of dyes and its rate of removal are found to increase with temperature (Table 9), indicating the process to be endothermic in nature. The half-life of the adsorption process ( $t_{50}$ ) decreases with an increase in the temperature. The amount of dyes removed in the first hour of contact increases as the temperature increases. The kinetics of the removal of MB and MO has also been studied at different concentrations (plots omitted for brevity). The amount of dye removed in the first hour of contact increases with an increase in the concentration of dye, and an increase in the initial concentration of dyes enhances the sorption rate. Further, the time required for 50% of the ultimate adsorption is found to be more or less independent of the initial adsorbate concentration (Table 9).

**Rate Constants.** The adsorption of dyes from the liquid to solid phase can be considered as a reversible reaction with equilibrium established between the two phases. The Lagergren first-order rate equation<sup>19,20</sup> (eq 9) can be applied for the determination of the rate constant. The data are shown as Lagergren plots in

$$\log(q_e - q_t) = \log q_e - (K_{\text{ad}}/2.303)t \quad (9)$$

Figure 12 to facilitate the analysis. A plot of  $\log(q_e - q_t)$  vs  $t$  gives a straight line, as can be seen in Figure

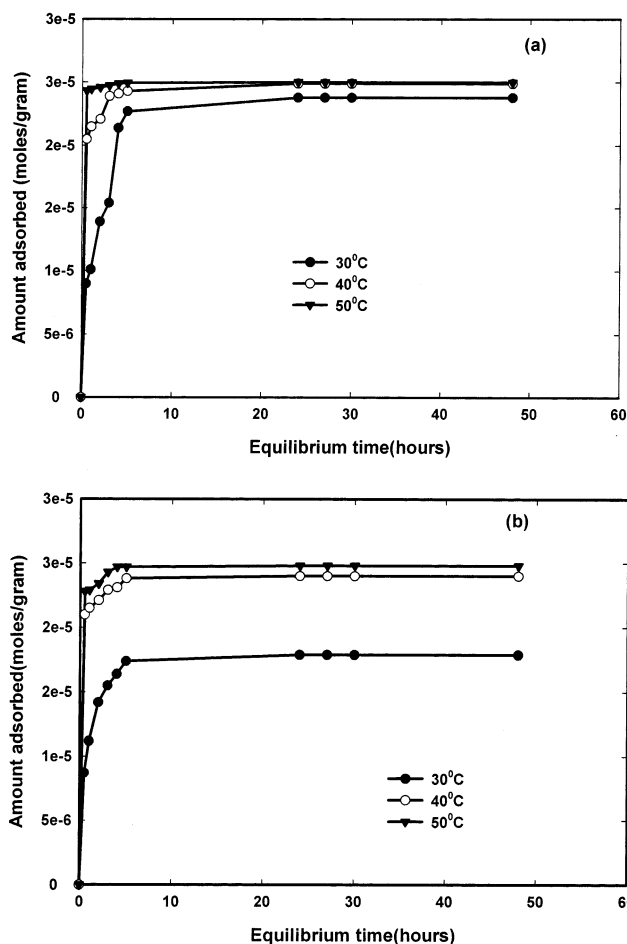


**Figure 11.** Effect of the temperature on the rate of adsorption of (a) MB and (b) MO on activated carbon derived from coconut shell fibers at pH 4.0 and 6.0, respectively, an adsorbent dose of 2 g/L, and an adsorbate concentration of  $5 \times 10^{-5}$  M.

**Table 8. Effect of the Temperature on the Rate of Uptake of MB and MO (Initial Concentration of the Dye,  $5 \times 10^{-5}$  M; Particle Size = 30–200 mesh) on Activated Carbon Prepared from Coconut Shell Fibers**

dye	temp ( $\pm 1$ °C)	amount adsorbed in the first hour (mol)	$t_{50}$ (h)
MB	30	$1.01 \times 10^{-5}$	1.2
	40	$2.15 \times 10^{-5}$	1.0
	50	$2.44 \times 10^{-5}$	<0.5
MO	30	$1.12 \times 10^{-5}$	0.8
	40	$2.15 \times 10^{-5}$	<0.5
	50	$2.29 \times 10^{-5}$	<0.5

**Table 9. Effect of the Adsorbate Concentration on the Rate of Uptake of MB and MO (Temperature =  $30 \pm 1$  °C; Particle Size = 30–200 mesh) on Activated Carbon Prepared from Coconut Shell Fibers**

dye	temp ( $\pm 1$ °C)	amount adsorbed in the first hour (mol)	$t_{50}$ (h)
MB	$1.00 \times 10^{-5}$	$4.8 \times 10^{-6}$	0.5
	$5.00 \times 10^{-5}$	$1.01 \times 10^{-5}$	1.2
	$10.00 \times 10^{-5}$	$1.7 \times 10^{-5}$	2.0
MO	$1.00 \times 10^{-5}$	$4.87 \times 10^{-6}$	0.8
	$5.00 \times 10^{-5}$	$1.12 \times 10^{-5}$	0.8
	$10.00 \times 10^{-5}$	$1.06 \times 10^{-5}$	1.0

12, confirming the applicability of the first-order Lagergren rate expression. The adsorption rate constants,  $K_{ad}$ , for MB and MO were calculated from the slope of the plots (Figure 12), and values are found to be  $9.68 \times 10^{-3}$ ,  $7.72 \times 10^{-3}$ , and  $9.40 \times 10^{-3}$  ( $R^2 =$

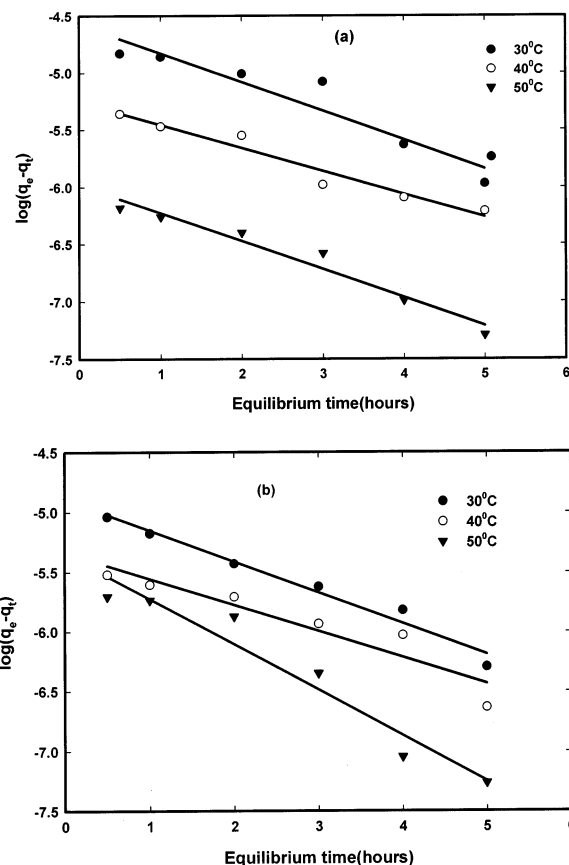


**Figure 12.** Lagergren plots for the adsorption of (a) MB and (b) MO on activated carbon at pH 4.0 and 6.0, respectively, an adsorbent dose of 2 g/L, and an adsorbate concentration of  $5 \times 10^{-5}$  M.

0.9015, 0.9536, and 0.9599) for MB and  $9.68 \times 10^{-3}$ ,  $9.68 \times 10^{-3}$ , and  $9.68 \times 10^{-3}$  ( $R^2 = 0.9744$ , 0.8914, and 0.9427) for MO at 30, 40, and 50 °C, respectively.

**Rate Mechanism.** Further, to interpret the experimental data, it is necessary to identify the step that governs the overall removal rate in the adsorption process. The mathematical treatment of Boyd et al.<sup>42</sup> and Reichenberg<sup>43</sup> to distinguish between the particle, film diffusion, and mass-action-controlled mechanism of exchange have laid the foundations of sorption/ion-exchange kinetics. The three consecutive steps in the adsorption of an organic/inorganic species by a porous adsorbent are as follows: (i) transport of the adsorbate to the external surface of the adsorbent (film diffusion); (ii) transport of the adsorbate within the pores of the adsorbent except for a small amount of adsorption that occurs on the external surface (particle diffusion); (iii) adsorption of the adsorbate on the exterior surface of the adsorbent.

It is generally accepted that process iii is very rapid and does not represent the rate-determining step in the uptake of organic/inorganic compounds.<sup>34</sup> For the remaining two steps in the overall transport, three distinct cases occur: case I, external transport > internal transport; case II, external transport < internal transport; case III, external transport  $\approx$  internal transport.

In cases I and II, the rate is governed by film and particle diffusion, respectively. In case III, the transport of ions to the boundary may not be possible at a significant rate, thereby leading to the formation of a liquid film with a concentration gradient surrounding the sorbent particles.

**Table 10. Effective Diffusion Coefficient ( $D_i$ ),  $D_0$ ,  $E_a$ , and  $\Delta S^\ddagger$  Values for the Diffusion of MB and MO in Activated Carbon Derived from Coconut Shell Fibers**

dye	effective diffusion coefficient ( $D_i$ ) (m <sup>2</sup> /s)			$D_0$ (m <sup>2</sup> /s)	$E_a$ (kJ/mol)	$\Delta S^\ddagger$ [J/(K mol)]
	30 °C	40 °C	50 °C			
MB	$2.38 \times 10^{-10}$	$2.98 \times 10^{-10}$	$3.08 \times 10^{-10}$	$1.56 \times 10^{-8}$	10.46	-46.62
MO	$2.92 \times 10^{-10}$	$3.28 \times 10^{-10}$	$3.74 \times 10^{-10}$	$1.54 \times 10^{-8}$	10.00	-46.75

Usually, external transport is the rate-limiting step in systems, which have (a) poor mixing, (b) dilute concentration of adsorbate, (c) small particle size, and (d) high affinity of the adsorbate for adsorbent. In contrast, the intraparticle step limits the overall transfer for those systems that have (a) high concentration of adsorbate, (b) good mixing, (c) large particle size of adsorbent, and (d) low affinity of the adsorbate for adsorbent.

Kinetic data were analyzed by the procedure given by Reichenberg<sup>43</sup> and Helfferich<sup>44</sup> using eqs 10–13

$$F = 1 - \frac{6}{\pi^2} \sum_{n=1}^{\infty} \frac{1}{n^2} \left[ \frac{-D_i t \pi^2 n^2}{r_0^2} \right] \quad (10)$$

or

$$F = 1 - \frac{6}{\pi^2} \sum_{n=1}^{\infty} \frac{1}{n^2} \exp[-n^2 Bt] \quad (11)$$

where  $F$  is the fractional attainment of equilibrium at time  $t$  and is obtained by the expression

$$F = Q_t / Q^0 \quad (12)$$

where  $Q_t$  is the amount of adsorbate taken up at time  $t$  and  $Q^0$  is the maximum equilibrium uptake and

$$B = \pi^2 D_i / r_0^2 = \text{time constant} \quad (13)$$

where  $D_i$  is the effective diffusion coefficient of the dye molecule in the adsorbent phase,  $r_0$  is the radius of the adsorbent particle, assumed to be spherical, and  $n$  is an integer that defines the infinite series solution.

The  $Bt$  values were obtained for each observed value of  $F$ , from Reichenberg's table,<sup>43</sup> and the results are plotted in Figure 13. The linearity test of  $Bt$  versus time plots was employed to distinguish between the film-diffusion- and particle-diffusion-controlled adsorption. If the plot of  $Bt$  vs time (having slope  $B$ ) is a straight line passing through the origin, then the adsorption rate is governed by the particle diffusion mechanism; otherwise, it is governed by film diffusion. For MB the plots are nonlinear and do not pass through the origin, indicating the film diffusion mechanism at low and higher concentrations. In the case of MO, an interesting nature of the plots was obtained. As can be seen from Figure 13, the plot at low concentration (i.e.,  $1 \times 10^{-5}$  M) is linear and does not pass through the origin, indicating the film diffusion mechanism, while at higher concentrations, i.e.,  $\geq 5 \times 10^{-5}$  M, the plots are linear and also pass through the origin, indicating the rate-controlling step to be particle diffusion. McKay plots at different adsorbate concentrations (plots are not provided in the manuscripts) further substantiated these findings. The effective diffusion coefficients at 30, 40, and 50 °C were also calculated and are given in Table 10. The increased mobility of ions and a decrease in the

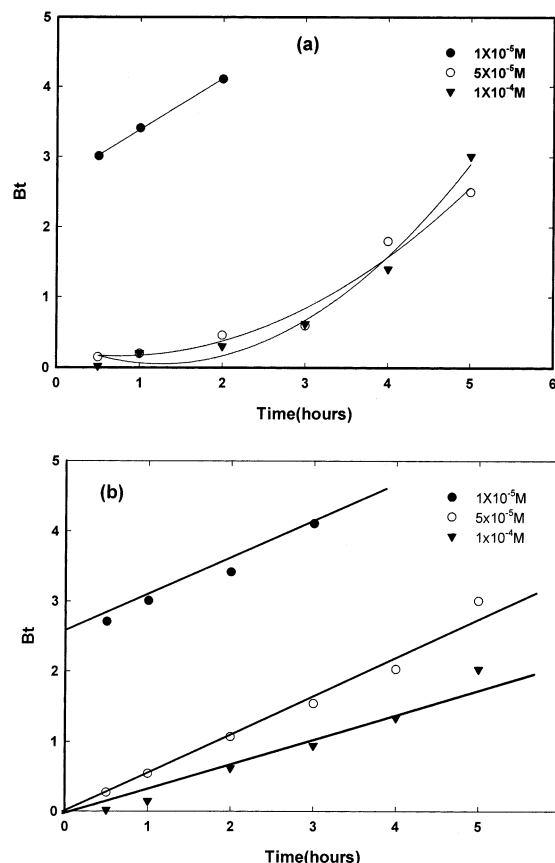


**Figure 13.**  $Bt$  vs time plots for the adsorption of (a) MB and (b) MO on activated carbon derived from agricultural waste material at different adsorbate concentrations.

retarding forces acting on the diffusing ion result in the increase of  $D_i$  with temperature (Figure 14). The energy of activation  $E_a$ , the entropy of activation  $\Delta S^\ddagger$ , and preexponential factor  $D_0$  analogous to the Arrhenius frequency factor were also evaluated using eqs 14 and 15 where  $k$  = Boltzmann's constant,  $h$  = Planck's

$$D_i = D_0 \exp(-E_a/RT) \quad (14)$$

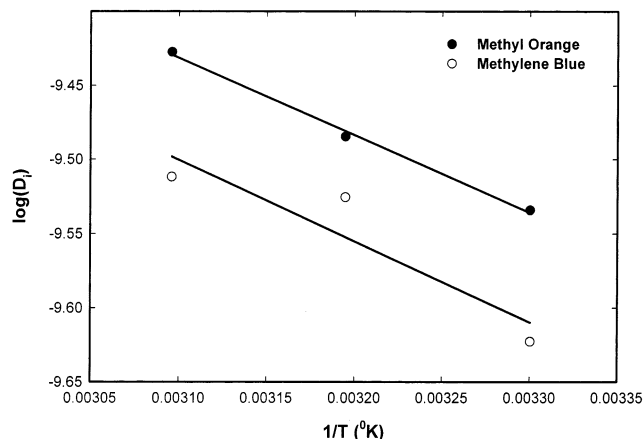
$$D_0 = 2.72 d^2 (kT/h) \exp(\Delta S^\ddagger/R) \quad (15)$$

constant,  $R$  = gas constant, and  $d$  = distance between two active sites of the adsorbent, which is conventionally taken as 5 Å. The values of  $E_a$ ,  $D_0$ , and  $\Delta S^\ddagger$  for the diffusion of MB and MO in activated carbon are also given in Table 10. The negative  $\Delta S^\ddagger$  values obtained for the adsorption of MB and MO on activated carbon reflect that no significant change occurs in the internal structure of the adsorbent material during adsorption. The negative  $\Delta S^\ddagger$  values are not uncommon in adsorption, and Gupta et al.<sup>19</sup> and Mohan and Singh<sup>34</sup> have also reported negative  $\Delta S^\ddagger$  values.

**3.6. Cost Estimation.** In India the cheapest variety of commercially available carbon costs US\$2.0/kg. The coconut shell fiber, a waste material, is available free

**Table 11. Adsorption Capacities of Cationic Dyes on Various Adsorbents**

name of the dye	low-cost adsorbents	adsorption capacity (mol/g)	ref
crystal violet	Wollastonite	$2.17 \times 10^{-6}$	41
Malachite green	blast furnace slag	$10.52 \times 10^{-5}$	19
Malachite green	activated carbon developed from fertilizer waste	$12.50 \times 10^{-5}$	19
MB	fly ash	$14.4 \times 10^{-5}$	40
MB	Perlite (EP)	$4.65 \times 10^{-5}$ – $8.21 \times 10^{-5}$	25
crystal violet	fly ash	$9.76 \times 10^{-5}$	30
Rosaniline hydrochloride or Basic Fuchsin	fly ash	$1.35 \times 10^{-5}$	30
MB	activated carbon derived from coconut shell fibers	$5.24 \times 10^{-5}$	this study
MO	activated carbon derived from coconut shell fibers	$2.88 \times 10^{-5}$	this study

**Figure 14.**  $\log D_i$  versus  $1/T$  plots for MB and MO adsorption on activated carbon prepared from coconut shell fibers.

of cost. When the total expenses for transport, chemicals, electrical energy, etc., are added up, the finished product would cost approximately US\$0.62/kg. Besides, the adsorbents can also be chemically regenerated (column studies are in progress) with simultaneous recovery of the adsorbate material, which would further bring down the cost of the activated carbon prepared from coconut shell fibers (column studies are in progress).

**3.7. Conclusions.** An activated carbon was prepared from coconut shell fibers, characterized, and utilized for the removal of MB and MO from wastewater in single and binary systems. The studies presented revealed that the adsorption of the two dyes increases with an increase in the temperature, thereby indicating the process to be endothermic. The results indicate that both the Freundlich and Langmuir models could be used to fit the data and estimate model parameters. Overall, the data are better fitted with the nonlinear Freundlich adsorption isotherm. The removal of both of the dyes is 100% at low concentration, while the same decreases with an increase in the concentration. The sorption capacity of the developed carbon is comparable to those of the other available adsorbents (Table 11), and cost-wise it is quite cheaper. The column studies as well as the regeneration of the adsorbent without dismantling the same are in progress to determine the fixed-bed parameters necessary for establishing the treatment plant. The studies presented revealed that the derived activated carbon could be fruitfully employed as an adsorbent for dye removal.

### Acknowledgment

The authors are thankful to the Director, Industrial Toxicology Research Centre, Lucknow, for providing all

necessary facilities for this work and consistent encouragement and guidance throughout the studies.

### Literature Cited

- (1) McKay, G.; Otterburn, M. S.; Sweeney, A. G. Surface Mass Transfer Processes During Color Removal from Effluent Using Silica. *Water Res.* **1981**, *115*, 327.
- (2) Reid, R. Go Green—a Sound Business Decision (part I). *J. Soc. Dyers Colour.* **1996**, *112*, 103.
- (3) Churchley, J. H. Removal of Dye Wastewater Color from Sewage Effluent—The Use of Full-Scale Ozone Plant. *Water Sci. Technol.* **1994**, *30* (3), 275.
- (4) Stephenson, R. J.; Sheldon, J. B. Coagulation and Precipitation of a Mechanical Pulp Mill Effluent: 1—Removal of Carbon and Turbidity. *Water Res.* **1996**, *30* (4), 781.
- (5) Coro, E.; Laha, S. Color removal in ground water through enhanced softening process. *Water Res.* **2001**, *35* (7), 1851.
- (6) Salem, I. A.; El-maazawi, M. Kinetics and mechanism of color removal of methylene blue with hydrogen peroxide catalysed by some supported alumina surfaces. *Chemosphere* **2000**, *41*, 1173.
- (7) Lee, V. K. C.; Porter, J. F.; McKay, G. Development of fixed-bed adsorber correlation model. *Ind. Eng. Chem. Res.* **2000**, *39*, 2427–2433.
- (8) Chern, J.-M.; Wu, C.-y. Desorption of dye from activated carbon beds: effects of temperature, pH and alcohol. *Water Res.* **2001**, *35* (17), 4259–4165.
- (9) Walker, G. M.; Weatherley, L. R. Adsorption of Acid Dyes on to Granular Activated Carbon in Fixed Beds. *Water Res.* **1997**, *31* (8), 2093.
- (10) Walker, G. M.; Weatherley, L. R. Fixed Bed Adsorption of Acid Dyes onto Activated Carbon. *Environ. Pollut.* **1998**, *99*, 133.
- (11) Meshko, V.; Markovska, L.; Mincheva, M.; Rodrigues, A. E. Adsorption of basic dyes on granular activated carbon and natural zeolite. *Water Res.* **2001**, *35* (14), 3357–3366.
- (12) Handreck, G. P.; Smith, T. D. Adsorption of Methylene Blue from Aqueous Solutions by ZSM-5-Type Zeolites and Related Silica Polymorphs. *J. Chem. Soc., Faraday. Trans 1* **1988**, *81* (11), 4191.
- (13) Allen, S. J.; McKay, G.; Khader, K. Y. H. Multicomponent Sorption Isotherms of Basic Dyes on Peat. *Environ. Pollut.* **1988**, *52* (1), 39.
- (14) McKay, G.; Allen, S. J.; McConvey, I. F.; Otterburn, M. Transport Processes in the Sorption of Colored Ions by Peat Particles. *J. Colloid Interface Sci.* **1981**, *80* (2), 323.
- (15) Al Duri, B.; McKay, G.; El Geundi, M. S.; Wahab Abdul, M. Z. Three Resistance Transport Model for Dye Adsorption onto Bagasse Pitch. *J. Environ. Eng. (N.Y.)* **1990**, *116*, 487.
- (16) McKay, G.; Otterburn, M. S.; Aga, J. A. Fuller's Earth and Fired Clay as Adsorbents for Dyestuffs—Equilibrium and Rate Studies. *Water, Air, Soil Pollut.* **1994**, *24*, 307.
- (17) Allen, S. J.; McKay, G.; Khader, K. Y. H. Equilibrium Adsorption Isotherms for Basic Dyes onto Lignite. *J. Chem. Technol. Biotechnol.* **1989**, *45*, 291.
- (18) Mittal, A. K.; Venkobachar, C. Sorption and Desorption of Dyes by Sulfonated Coal. *J. Environ. Eng. (N.Y.)* **1993**, *119*, 366.
- (19) Gupta, V. K.; Srivastava, S. K.; Mohan, D. Equilibrium Uptake, Sorption Dynamics, Process Optimization and Column Operation for the Removal and Recovery of Malachine Green from



Wastewater using Activated Carbon and Activated Slag. *Ind. Eng. Chem. Res.* **1997**, 36 (6), 2207.

(20) Gupta, V. K.; Mohan, D.; Sharma, S.; Sharma, M. Removal of Basic Dyes (Rhodamine-B and Methylene Blue) from Aqueous Solutions using bagasse fly ash. *Sep. Sci. Technol.* **2000**, 35 (13), 2097.

(21) Pelekani, C.; Snoeyink, V. L. A kinetic and equilibrium study of competitive adsorption between atrazine and cango red dye on activated carbon. *Carbon* **2001**, 39, 25.

(22) Perinea, F.; Molinier, J.; Gaset, A. Adsorption of Ionic Dyes on Wool Carbonizing Waste. *Water Res.* **1983**, 117, 559.

(23) Khare, S. K.; Srivastava, R. M.; Panday, K. K.; Singh, V. N. Removal of Basic Dye (Crystal Violet) from Waste Water using Wollastonite as Adsorbent. *Environ. Technol.* **1989**, 10, 785.

(24) Judkins, J. F.; Homsby, J. S. Colour Removal from Textile Dye Waste Using Magnesium Carbonate. *J. Water Pollut. Control Fed.* **1978**, 2246.

(25) Dogan, M.; Mahir, A.; Onganer, Y. Adsorption of Methylene Blue from Aqueous Solution onto Perlite. *Water, Air, Soil Pollut.* **2000**, 120, 229.

(26) McKay, G.; Alexander, F. Kinetics of the Removal of Basic Dye from Effluent Using Silica. *Chem. Eng.* **1977**, Apr, 234.

(27) McKay, G.; McConvey, I. F. Adsorption of Acid Dye onto Wood Meal by Solid Diffusion Mass Transfer. *Chem. Eng. Process.* **1995**, 19, 285.

(28) Wu, F.-C.; Tseng, R.-L.; Juang, R.-S. Preparation of Activated Carbons from Bamboo and their Adsorption Abilities from Dyes and Phenol. *J. Environ. Sci. Health.* **1999**, 34 (9), 1753.

(29) Chu, W. Dye removal from textile dye wastewater using recycled alum sludge. *Water Res.* **2001**, 35 (13), 3147.

(30) Mohan, D.; Singh, K. P.; Singh, G.; Kumar, K. Removal of dyes from wastewater using fly ash-a low cost adsorbent. *Ind. Eng. Chem. Res.* **2002**, 41, 3688–3695.

(31) Viraraghavan, T.; Ramakrishna, K. R. Fly ash for colour removal from synthetic dye solutions. *Water Qual. Res. J. Can.* **1999**, 34 (3), 505.

(32) Lambert, S. D.; Graham, N. J. D. Adsorption Methods for Treating Organically Colored Upland Waters. *Environ. Technol.* **1989**, 10, 785.

(33) Delee, V.; O'Neill, C.; Hawkes, F. R.; Pinheiro, H. M. Anaerobic Treatment of Textile Effluents: a Review. *J. Chem. Technol. Biotechnol.* **1998**, 73, 323.

(34) Mohan, D.; Singh, K. P. Single and multicomponent adsorption of cadmium and zinc using activated carbon derived from bagasse-an agricultural waste. *Water Res.* **2002**, 36, 2304.

(35) Sivasamy, A.; Singh, K. P.; Mohan, D.; Maruthamuthu, M. Studies on defluoridation of water by coal-based sorbents. *J. Chem. Technol. Biotechnol.* **2001**, 76, 717–722.

(36) Mohan, D.; Chander, S. Single Component and Multicomponent Metal Ions Adsorption by Activated Carbons. *Colloids Surf. A* **2001**, 177, 183.

(37) Vogel, A. I. *A Textbook of Quantitative Chemical Analysis*, 5th ed.; ELBS Publication: London, England, 1989.

(38) McKay, G. *Use of Adsorbents for the Removal of Pollutants from Wastewaters*; CRC Press: Boca Raton, FL, 1995.

(39) Weber, W. J., Jr. *Physical Process for Water Quality Control*; Wiley Interscience: New York, 1972.

(40) Weber, T. W.; Chackravorty, R. K. Pore and Solid Diffusion Models for Fixed Bed Adsorbents. *J. Am. Inst. Chem. Eng.* **1974**, 20, 228.

(41) Khare, S. K.; Srivastava, R. M.; Panday, K. K.; Singh, V. N. Removal of basic dye (crystal violet) from water using wollastonite as adsorbent. *Environ. Technol. Lett.* **1988**, 9, 1163.

(42) Boyd, G. E.; Adamson, A. W.; Mayers, L. S. The exchange adsorption of ions from aqueous solution by organic zeolites. II. Kinetics. *J. Am. Chem. Soc.* **1947**, 69, 2836.

(43) Reichenberg, D. Properties of Ion-exchange resin in relation to their structure. III. Kinetics of Exchange. *J. Am. Chem. Soc.* **1953**, 75, 589.

(44) Helfferich, F. *Ion Exchange*; McGraw-Hill Book Co., Inc.: New York, 1962.

Received for review October 10, 2002

Revised manuscript received January 17, 2003

Accepted February 6, 2003

IE020800D